Pivotal role for α_V integrins in sustained Tfh support of the germinal center response for long-lived plasma cell generation

Dillon C. Schrock[a,1], Scott A. Leddon[a,1], Angela Hughson[a], Jim Miller[a], Adam Lacy-Hulbert[b], and Deborah J. Fowell[a,2]

[a]David H. Smith Center for Vaccine Biology and Immunology, Department of Microbiology and Immunology, University of Rochester Medical Center, Rochester, NY 14642; and [b]Immunology Program, Benaroya Research Institute, Seattle, WA 98101

Edited by Jason G. Cyster, University of California, San Francisco, CA, and approved January 15, 2019 (received for review May 30, 2018)

CD4+ follicular helper T cells (Tfh) are essential for germinal center (GC) reactions in the lymph node that generate high-affinity, long-lived plasma cells (LLPCs). Temporal GC analysis suggests B memory cells (Bmem) are generated early, while LLPCs are generated late in the GC reaction. Distinct roles for Tfh at these temporally different stages are not yet clear. Tfh entry into the GC is highly dynamic and the signals that maintain Tfh within the GC for support of late LLPC production are poorly understood. The GC is marked by inflammation-induced presentation of specific ECM components. To determine if T cell recognition of these ECM components played a role in Tfh support of the GC, we immunized mice with a T cell-restricted deletion of the ECM-binding integrin α_V (α_V-CD4 cKO). T cell integrin α_V deletion led to a striking defect in the number and size of the GCs following immunization with OVA protein in complete Freund's adjuvant. The GC defect was not due to integrin α_V deficiency impeding Tfh generation or follicle entry or the ability of α_V-CD4 cKO Tfh to contact and support B cell activation. Instead, integrin α_V was essential for T cell-intrinsic accumulation within the GC. Altered Tfh positioning resulted in lower-affinity antibodies and a dramatic loss of LLPCs. Influenza A infection revealed that α_V integrin was not required for Tfh support of Bmem but was essential for Tfh support of LLPCs. We highlight an α_V integrin–ECM-guided mechanism of Tfh GC accumulation that selectively impacts GC output of LLPCs but not Bmem.

germinal center | T follicular helper | integrin | ECM | LLPC

The development of long-term, high-affinity humoral immunity is a key feature of protective immunity and the ultimate goal of effective vaccine strategies (1). The germinal center (GC) reaction is initiated following infection or immunization and supports the development of high-affinity antibody responses (2–4). Within GCs, B cells undergo repeated cycling between the dark zone (DZ), where somatic hypermutation (SHM) and proliferation occur, and the light zone (LZ), where they acquire antigen from follicular dendritic cells (FDCs) and compete for T cell help (5–8). Follicular helper T cells (Tfh) provide T cell help in the LZ that licenses B cells for further rounds of affinity maturation, resulting in high-affinity antibodies and the establishment of long-lived immunity (9, 10). Competition for Tfh help is required for continued B cell proliferation and SHM in the DZ (11, 12), while excess Tfh lead to aberrant autoantibody production and autoimmunity (13). Thus, regulation of Tfh numbers is critical for selective pressure on GC B cell affinity maturation.

The GC is a dynamic microanatomical structure under tight spatiotemporal control (7, 12). Both B and T cells utilize G protein-coupled receptor signals to locate at the T:B cell border for cognate T:B cell interactions. Down-regulation of CCR7 and up-regulation of CXCR5 facilitate Tfh recruitment to the CXCL13-enriched follicle (14, 15). Continued cognate T:B cell interactions are critical for GC development, as highlighted by the failed GC response when T cells lack SAP (16, 17), and in GC maintenance, as demonstrated on CD40/CD40L blockade (18–20). Restriction of Tfh and B cells to GCs is controlled in part by S1PR2 expression (21, 22), which inhibits responsiveness to the sphingosine-1-phosphate (S1P) gradient that draws Tfh out of GCs. Contact-dependent mechanisms involving EPH/ephrin B1 interactions (23) and the plexin B2–semaphorin 4C axis (24) have also been implicated in Tfh GC positioning. However, the overall impact of these individual molecular Tfh positional cues on GC function was modest and the impact on long-lived plasma cells (LLPCs) GC output not fully addressed. Therefore, despite recent advances, critical mechanisms that regulate Tfh retention in the GC LZ for provision of GC B cell help remain unclear.

Inflammation can drive marked changes in composition and organization of the ECM (25). The lymph node (LN) ECM in the T cell zone is thought to primarily reside as reticular fibers ensheathed in a layer of fibroblastic reticular cells (FRCs) (26), although some ECM may be accessible to lymphocytes (27). Distinct ECM patterning in GCs has been observed, with a number of Arg-Gly-Asp (RGD)-containing ECM ligands colocalizing with FDCs (28–31). However, the GC response remained largely intact when B cells lacked integrin receptors for these ligands (29). RGD-containing ECM components are known to be strong ligands for the α_V integrin family. These α_V integrins are functionally important for macrophages, dendritic cells, B cells, and T cells, where they regulate processes such as apoptotic clearance

Significance

The hallmark of protective immunity to infection and vaccination is the generation of long-lived plasma cells (LLPCs) secreting high-affinity antibodies. T follicular helper cells (Tfh) must be retained within specialized germinal center (GC) structures to provide essential help to B cells for LLPC generation. How such Tfh GC accumulation is sustained is unclear. We identify an ECM:α_V integrin axis in the control of the GC reaction. In the absence of T cell α_V integrins, Tfh are generated and can support early B cell responses but fail to accumulate within the GC, resulting in a striking absence of LLPCs. Targeting α_V integrins may enable novel therapeutic control of Tfh GC numbers to boost immunity or mitigate Ab-mediated autoimmune pathology.

Author contributions: D.C.S., S.A.L., J.M., A.L.-H., and D.J.F. designed research; D.C.S., S.A.L., and A.H. performed research; A.L.-H. contributed new reagents/analytic tools; D.C.S., S.A.L., A.H., and D.J.F. analyzed data; and D.C.S., S.A.L., and D.J.F. wrote the paper.

The authors declare no conflict of interest.

This article is a PNAS Direct Submission.

[1]D.C.S. and S.A.L. contributed equally to this work.

[2]To whom correspondence should be addressed. Email: deborah_fowell@urmc.rochester.edu.

This article contains supporting information online at www.pnas.org/lookup/suppl/doi:10.1073/pnas.1809329116/-/DCSupplemental.

Published online February 15, 2019.

(32, 33), TGF-β activation (34–36), Toll-like receptor signal strength (37–39), and cell migration (40, 41).

Here we describe a critical, nonredundant role for integrin α_V in Tfh support of the GC response. Conditional deletion of integrin α_V in T cells (CD4-Cre) led to a striking defect in GCs and the absence of LLPCs. This α_V-CD4 cKO phenotype was not due to a failure to differentiate into Tfh. Moreover, in contrast to the failure to sustain T:B interactions with SAP deficiency (16), integrin α_V-deficient Tfh were capable of forming T:B conjugates and providing B cell help. Instead, the inability of Tfh cells to bind RGD-containing ligands in the GC led to a failure of α_V-deficient Tfh cells to localize within GCs. Tfh mislocalization to the B cell follicle did not impact early B cell activation or initial memory B cell (Bmem) formation, but did result in the marked absence of LLPC in the bone marrow (BM). Our studies reveal that T cell integrin α_V plays a pivotal role in prolonged Tfh support of GC formation for the generation of high-affinity LLPCs.

Results

RGD-Containing ECM Components Mark the GC. Previous reports of spatially restricted ECM in GCs (42) promoted further analysis of ECM distribution in inflamed LNs. Mice were immunized with OVA protein in complete Freund's adjuvant (OVA/CFA) to induce a robust T-dependent B cell response and the draining LNs (dLN) were isolated and evaluated for ECM display by immunohistochemistry (IHC). Fibronectin (FN), the canonical integrin α_V RGD-containing ligand, was distributed throughout the LN medulla coincident with the podoplanin$^+$ reticular cells (43) and was underrepresented in the B cell follicle (Fig. 1 *A* and *D*) (see *SI Appendix*, Fig. S1 for B220 counterstain). FN distribution and expression level did not change following inflammation (Fig. 1*B*). In contrast, a number of RGD-containing ligands [vitonectin (VN), MFG-E8, and osteopontin (OPN)] were enriched in the GC upon immunization (Fig. 1 *A*–*D*). VN colocalized with a subset of the CD35+ FDCs (Fig. 1*E*), coincident with GL7$^+$ GC structures (*SI Appendix*, Fig. S1), as previously described (28, 29). VN increased with inflammation and remained high 30 d postimmunization (Fig. 1*B*). RGD-containing ligands MFG-E8 and OPN were also strongly associated with the FDC network (Fig. 1 *C* and *D*) and in proximity to follicular CD4 T cells (Fig. 1*D*). Confocal imaging confirmed close association between T cells, FDC, and VN in GL7$^+$ areas (Fig. 1*E*; see *SI Appendix*, Fig. S1 for LN position). Three-dimensional surface reconstruction enabled unbiased assessment of surface overlap between interacting cells (white, Fig. 1*E*): ~76% of T cells were in contact with FDC and of them 80% were coincident with VN.

Impaired GC Development in Mice Lacking T Cell Expression of Integrin α_V. To determine whether T cell binding to GC-enriched RGD-containing ECM components is important for the GC reaction, we conditionally deleted integrin α_V in T cells with CD4-Cre, *itgav*$^{fl/fl}$ CD4-Cre$^+$ (designated α_V-CD4 cKO). Deletion of integrin α_V in T cells did not alter the number of T and B cells in the steady state (*SI Appendix*, Fig. S2). WT and α_V-CD4 cKO mice were immunized with OVA/CFA and GC morphology in the dLN assessed histologically days 14, 21, and 28–30 after immunization (Fig. 2). GCs were defined based on GL7$^+$ staining within the B220$^+$ follicle. For WT controls, $\alpha_V^{+/+}$ CD4-Cre$^+$ littermates and C57BL/6 (JAX) were used interchangeably (see the summary of results for both control groups in *SI Appendix*, Fig. S11). In the absence of T cell α_V integrin, GCs were formed by day 14 (Fig. 2), but by day 28 GCs were significantly reduced in number and size compared with WT (Fig. 2 *A*–*C*) and were also less dense (as measured by the integrated density of GL7 staining in GL7$^+$ areas; Fig. 2*D*). These results support a nonredundant role for α_V integrin expression by CD4+ T cells in the maintenance of the GC reaction following immunization.

Tfh Development Occurs Independently of α_V Integrin Expression. Tfh differentiation is initiated with T cell-zone dendritic cells and completed by subsequent interactions with activated B cells. The

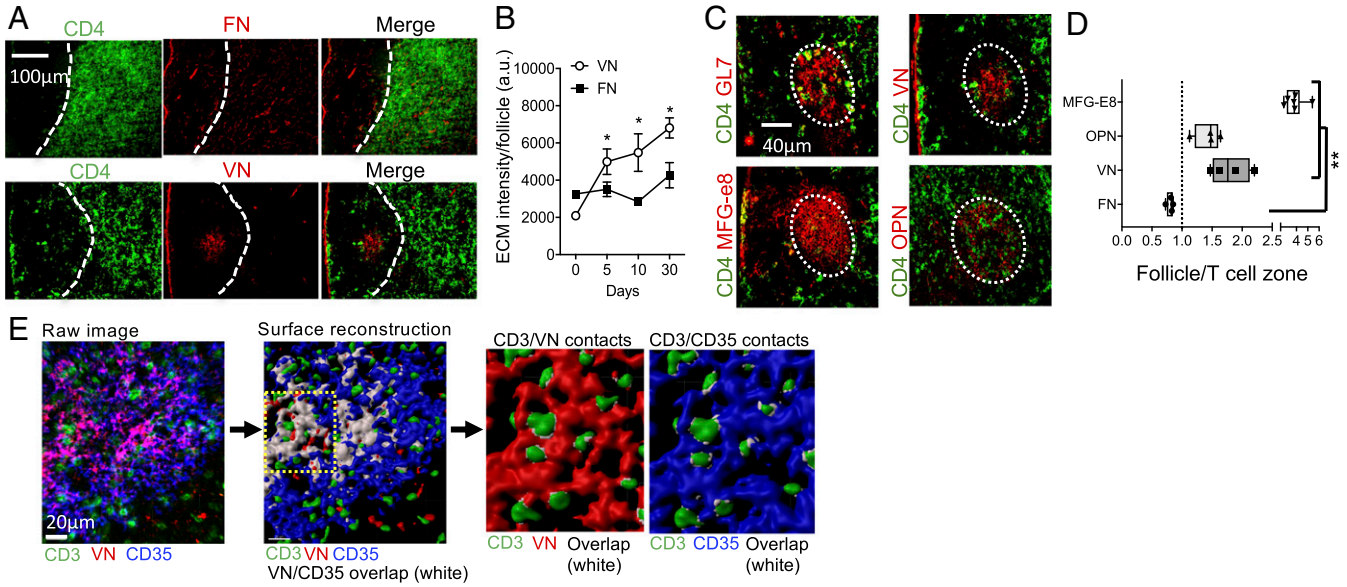

Fig. 1. GC-enriched RGD-containing ECM components. (*A*–*D*) IHC of dLN 30 d after OVA/CFA immunization of WT C57BL/6 mice. (*A*) FN and VN relative to CD4$^+$ T cells. Dotted line, T:B cell boarder [based on CD4 and B220 (*SI Appendix*, Fig. S1) staining]. (*B*) Quantitation of FN and VN in the B220$^+$ follicles following OVA/CFA immunization; total integrated density for the entire follicle area. (*C*) Serially sectioned dLN for CD4 T cells and GL7 and ECM proteins in the same follicle; VN, milk fat globulin E8 (MFG-E8), and OPN. (*D*) Ratio of ECM staining in the B220$^+$ follicle compared with that in an adjacent T cell zone area of similar size; symbols represent individual follicles. Representative data from one of at least three independent experiments: three to four mice per group per experiment. Statistics by two-tailed *t* test; $^*P < 0.05$, $^{**}P < 0.01$. (*E*) Confocal images of GL7$^+$ GC area of the dLN day 14 postimmunization of WT C57BL/6 mice (see *SI Appendix*, Fig. S1 for LN position), analyzed by creating 3D surfaces for each channel in Imaris (Bitplane); overlap displayed as an independent surface in white.

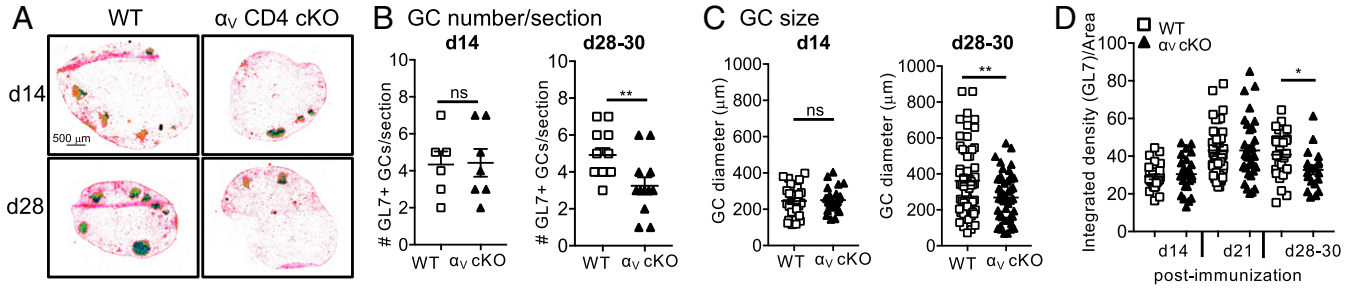

Fig. 2. T cell deficiency in α_V integrins results in impaired GC formation. (*A–D*) IHC of the dLN day 14 and days 28–30 after OVA/CFA immunization of WT (C57BL/6 and $\alpha_V^{+/+}$ CD4-Cre$^+$) or α_V-CD4 cKO mice. (*A*) GL7 staining to mark the GC; 4× colors reflect intensity of GL7 staining on a scale of blue (low) to red (high). (*B*) Number of GL7$^+$ GC per LN section from WT or α_V-CD4 cKO mice, day 14 and days 28–30 postimmunization. GL7$^+$ GC numbers per LN section (each symbol an individual mouse) shown as number of GL7$^+$ objects above 100 μm^2. (*C*) Size of GC day 14 and days 28–30 postimmunization; maximum diameter of all detected GL7$^+$ objects above 100 μm^2 (each symbol an individual GC). (*D*) Integrated density of GL7 staining for GL7$^+$ objects/areas above 100 μm^2. Two to five independent experiments, three to four mice per group/experiment. Statistics by Mann–Whitney *U* test; $*P < 0.05$, $**P < 0.01$. ns, not statistically significant.

integrin LFA-1 contributes to Tfh generation (44), but the role of integrin α_V in Tfh generation is unknown. Tfh cells express relatively low levels of integrin α_V compared with other CD44^{high} CD4$^+$ T cells (*SI Appendix*, Fig. S4), which may indicate that its function on these cells is highly sensitive to ligand density. To determine if integrin α_V is required for Tfh development, WT and α_V-CD4 cKO mice were immunized with OVA/CFA and dLN were analyzed by flow cytometry on day 10 for Tfh cells: PD1^{high}CXCR5^{high}CD44^{high} CD4$^+$ (Fig. 3*A*). Inducible costimulator (ICOS) expression, critical for Tfh differentiation and GC function (45, 46), and the Tfh transcriptional regulator Bcl6 were expressed similarly on Tfh cells from WT and α_V-CD4 cKO mice (*SI Appendix*, Fig. S5). Tfh from WT and α_V-CD4 cKO had also both down-regulated CCR7. Kinetically, the Tfh response peaked at day 14, with WT and α_V-CD4 cKO mice having similar numbers and frequencies of Tfh throughout the response (Fig. 3*B*). Similarly, the number of non-Tfh CD44^{high} CD4$^+$ cells expanded and contracted in response to immunization comparably (*SI Appendix*, Fig. S5). Analysis of Foxp3$^+$ regulatory Tfh (Tfr) (47, 48) from WT or α_V-CD4 cKO mice showed no difference in the size of this subset (*SI Appendix*, Fig. S5), suggesting aberrant Tfr generation cannot explain the diminished GC response. In addition, the generation of effector cytokines IFN-γ, IL-4, IL-17, and IL-21 from CD4$^+$ T cells was not altered in the α_V-CD4 cKO mice (*SI Appendix*, Fig. S6). Thus, T cell activation and Tfh/Th differentiation does not require T cell expression of integrin α_V.

Integrin α_V Is Dispensable for Tfh Help to B Cells. Initial T cell interactions with B cells are heavily dependent on SAP (16) and on the integrins LFA-1 and VLA-1 (17). In addition to their role in binding to the ECM, α_V integrins can function in adhesion and signaling during cell:cell interactions via cell-surface expression of RGD-containing molecules. Therefore, α_V integrins could play a role in initial T:B cell interactions and/or provision of help to B cells. To test this, we used both in vitro and in vivo assays of T:B conjugation and B cell activation. In contrast to published roles for LFA-1/VLA-1 in T:B interactions (17, 49), integrin α_V-deficient T cells readily formed conjugates with B cells in an antigen dose-dependent fashion in vitro (Fig. 4 *A* and *B*); thus, T cell integrin α_V is not required for initial cell:cell contact with B cells. We next asked if the in vivo-generated Tfh from α_V-CD4 cKO mice could provide help for B cell activation and IgG production. Naïve B cells were cocultured with FACS-purified Tfh from WT and α_V-CD4 cKO mice and analyzed for B cell maturation through induction of GL7 and production of IgG (Fig. 4 *C* and *D*). To determine if support of early B cell activation occurred in vivo, we set up an adoptive transfer system whereby the transferred T cells were the predominant source of antigen-specific T cell help. MOG-specific 2D2 TCR Tg$^+$ mice (unable to provide OVA-specific T cell help) were used as recipients of HEL-specific MD4 Tg$^+$ B cells with/without cotransfer of WT or α_V-CD4 cKO OVA-specific OT-II TCR Tg$^+$ cells. Recipient mice were immunized with HEL-OVA protein emulsified in CFA and the extent of early B cell expansion and maturation (loss of IgD and Bcl-6 induction) was measured day 5 postimmunization (see gating strategy in *SI Appendix*, Fig. S3). In the absence of T cell transfer, the 2D2 recipients failed to support B cell activation to OVA-HEL (Fig. 4 *E–G*). In contrast, both WT and α_V-CD4 cKO OT-II transfers provided robust help

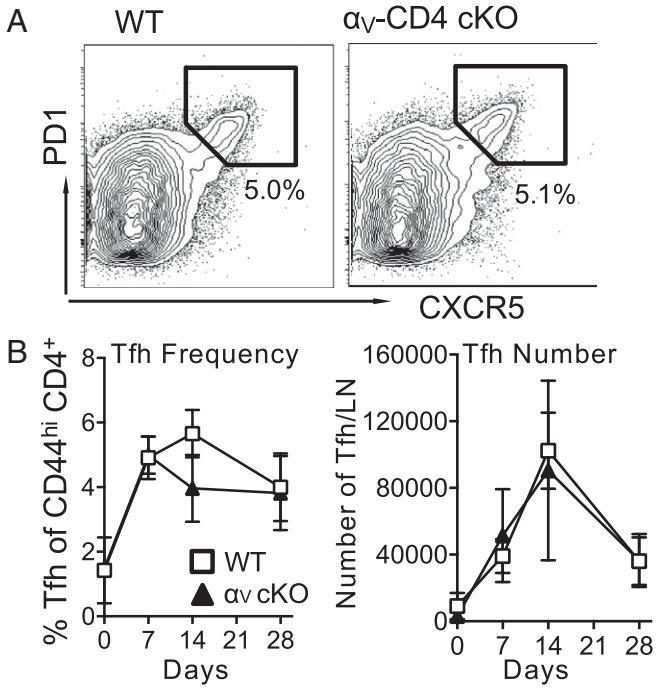

Fig. 3. Tfh cells develop independently of α_V integrin expression. Kinetic analysis of Tfh after OVA/CFA immunization. (*A*) CXCR5$^+$ PD1$^+$ Tfh cells, gated on CD4$^+$CD44^{high} cells (numbers, percentage of CD4$^+$CD44$^+$ cells that are PD1$^+$CXCR5$^+$). (*B*) Frequency (*Left*) and number per dLN (*Right*) gated as in *A* for WT (C57BL/6) and α_V-CD4 cKO mice. One representative experiment of three to six independent experiments, four to five mice per group/experiment. No significant differences between WT and α_V CD4 cKO by two-way ANOVA.

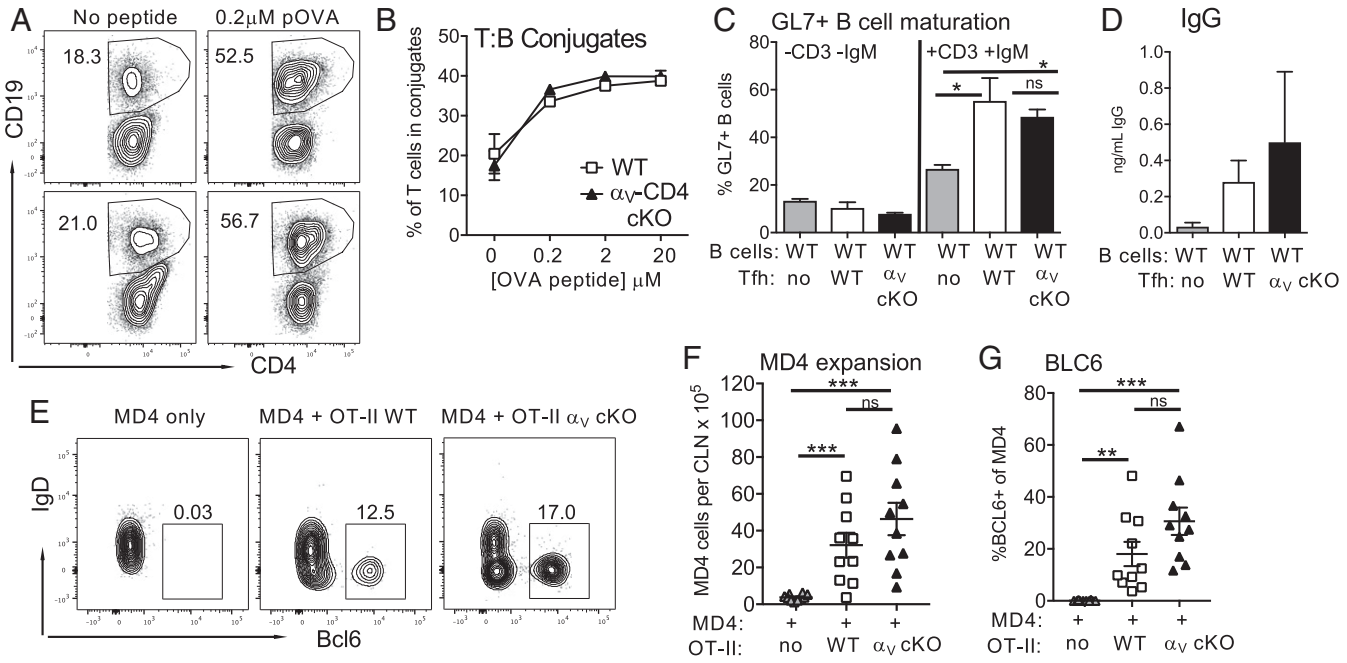

Fig. 4. Provision of B cell help by α_V-deficient Tfh. (*A* and *B*) Antigen-dependent T:B conjugation of WT OVA-loaded LPS-stimulated B cells with IL-2 cultured WT ($\alpha_V^{+/+}$ CD4-Cre$^+$) or α_V-CD4 cKO OTII CD4$^+$ T cells. (*A*) Representative FACS plots (numbers, percent of CD4 cells in conjugate with CD19 B cells). (*B*) Antigen-dose response. (*C*) B cell activation by Tfh. Resting B cells from naïve animals cultured with in vivo Tfh from day-10 OVA/CFA-immunized WT and α_V-CD4 cKO mice ± anti-CD3 and anti-IgM Abs. Percent CD19$^+$ CD4$^-$ GL7$^+$ B cells after 6 d of coculture. (*D*) IgG in supernatant of day-11 Tfh and B cell cocultures. (*A* and *B*) One of three independent experiments. (*C* and *D*) Mean of two to four individual experiments. Statistics by two-tailed *t* test; $*P < 0.05$. (*E–G*) In vivo B cell help assay: MDA transfer ± OT-II (C57BL/6) or OT-II α_V-CD4 cKO into 2D2-recipient mice followed by immunization with HEL-OVA/CFA. Analysis of MD4 expansion (*F*) and Bcl6 induction (*E* and *G*) day 5 postimmunization. (*E*) Representative FACS plots (numbers, percentage of MD4 cells IgD^{low}, Bcl6$^+$). Two independent experiments, five mice per group. Statistics by Mann–Whitney *U* test; $**P < 0.01$, $***P < 0.001$. ns, not statistically significant.

to B cells for expansion and Bcl-6 up-regulation (Fig. 4 *E–G*). Therefore, integrin α_V-deficient Tfh were comparable to WT Tfh in their help for B cells in vitro and in vivo, suggesting the loss of integrin α_V does not lead to inherent defects in initial T cell support of B cell activation.

Integrin α_V Is Required for Tfh Accumulation in the GC. Integrin α_V-CD4 cKO mice appear to generate Tfh and provide B cell help but nonetheless have defects in the maintenance of GC structures (Fig. 2). Given the spatially restricted presentation of α_V ligands by FDC, we asked whether the loss of integrin α_V changed the ability of Tfh to positioning correctly in the ECM-rich GC. IHC of LNs from WT animals 30 d after immunization showed significant infiltration of the GL7$^+$ GC by CD4$^+$ T cells (Fig. 5*A*). Where GCs did form in the α_V-CD4 cKO mice, CD4$^+$ T cell GC accumulation was dramatically reduced (Fig. 5*A*) (see additional images in *SI Appendix*, Fig. S7). Enumeration of CD4$^+$ T cells in B cell follicles and GCs indicated a selective defect in CD4$^+$ T cell accumulation in GCs in the absence of integrin α_V (Fig. 5*B*). Therefore, α_V-deficient CD4$^+$ T cells remain responsive to cues to enter the B cell follicle but their localization to GCs is selectively impaired. To further understand the temporal impact on Tfh accumulation in the GC, we also measured T cell GC accumulation in WT and α_V-CD4 cKO mice at an earlier time point, day 14 postimmunization. At this time, α_V-deficient Tfh were able to accumulate in the GC similarly to WT (Fig. 5*C*), which is consistent with the earlier findings that GC are present on day 14 but have collapsed by days 28–30 in α_V-CD4 cKO mice (Fig. 2). To directly test a T cell-intrinsic requirement for α_V integrin in Tfh localization to GCs we adoptively transferred either naïve OT-II WT or α_V-deficient CD4$^+$ T cells to WT mice followed by OVA/CFA immunization. Integrin α_V-deficient OT-II CD4$^+$ T cells homed to the LN, expanded following OVA/CFA immunization, and generated similar frequencies of Tfh in comparison with their WT counterparts (*SI Appendix*, Fig. S8). However, far fewer OT-II α_V-CD4 cKO CD4$^+$ T cells were found in the WT GC compared with WT OT-II cells (Fig. 5 *D* and *E*). Thus, there is a T cell-intrinsic requirement for α_V integrin in GC accumulation. We speculate that impaired Tfh retention in the GC in the absence of α_V integrin occurs throughout the course of the GC reaction, as highlighted by the adoptive transfer of a synchronized cohort of α_V-deficient OT-II T cells. At the polyclonal level, defects in GC retention are likely asynchronous and iterative, becoming functionally impactful late in the GC response, suggesting that defects in GC positioning are compounded with time, resulting in the observed late defect in Tfh GC association.

To independently assess the role of α_V integrin in Tfh GC accumulation we immunized WT mice, allowed the GCs to form, and then acutely blocked α_V integrins using the $\alpha_V\beta_3$ inhibitor cilengitide (41, 50, 51). WT mice were immunized with OVA/CFA and treated with cilengitide daily (100 μg i.p.) from days 17–20 postimmunization (Fig. 5*F*). LNs were examined by IHC for T cell localization within the GL7$^+$ GCs on day 21 postimmunization (Fig. 5*G*). Acute blockade of $\alpha_V\beta3$ led to a significant decrease in T cell localization within the GC (Fig. 5 *G* and *H*). Therefore, both genetic deletion of α_V integrin and acute blockade of α_V integrin in WT mice results in a selective defect in T cell GC accumulation.

Late Defect in the GC B Cell Response in Absence of Tfh α_V Integrin Expression. Since α_V-deficient Tfh poorly accumulate in the GC, we examined the development of the associated GC B cell response. Consistent with our structural GC analysis (Fig. 2), GC B cell numbers and frequency in the α_V-CD4 cKO mice were comparable to WT on days 7 and 14 but declined by days 28–30 (Fig. 6 *A–C*) (see gating strategies in *SI Appendix*, Fig. S3). We also tested B cell function by analysis of OVA-specific antibody secreting

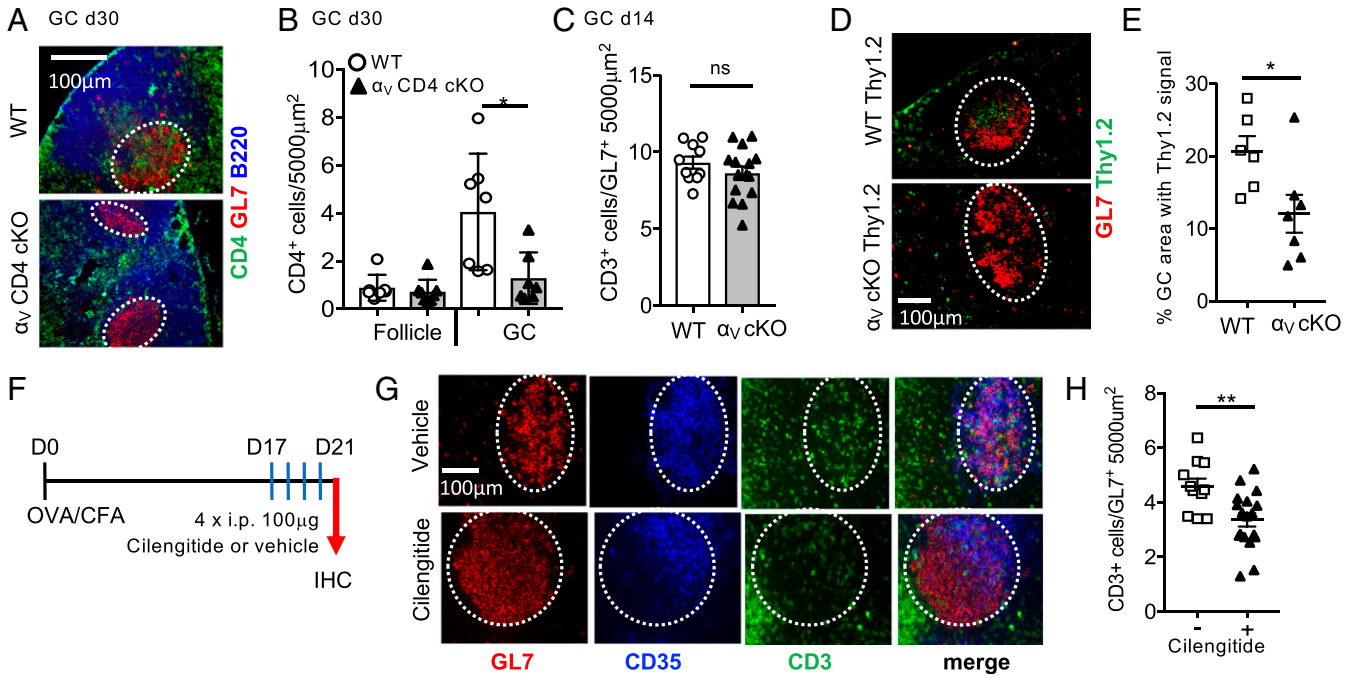

Fig. 5. Defect in Tfh localization to the GC in the absence of α_V integrins. (*A* and *B*) $CD4^+$ T cell localization in the dLN of WT ($\alpha_V^{+/+}$ CD4-Cre^+) and α_V-CD4 cKO mice day 30 after OVA/CFA immunization. (*A*) Representative IHC, $B220^+$ (blue) B cell follicles, $GL7^+$ (red) GCs, and $CD4^+$ (green) T cells. Dotted lines, approximate GC area. Similar distribution was noted when either anti-CD4 or anti-CD3 Abs was used to mark T cells in the GC; therefore, they have been used interchangeably. (*B*) $CD4^+$ objects within the $B220^+$ $GL7^-$ follicle and $B220^{low}$ $GL7^+$ GC, number per 5,000 μm^2. (*C*) $CD3^+$ objects within the $GL7^+$ GC, day 14 postimmunization. (*D* and *E*) WT($\alpha_V^{+/+}$ CD4-Cre^+) or α_V-CD4 cKO naïve OTII $Thy1.2^+$ T cells transferred to WT $Thy1.1^+$ mice and immunized with OVA/CFA. (*D*) IHC, $GL7^+$ (red) GCs, and $Thy1.2^+$ (green) transferred cells, day 10. (*E*) Fraction of $GL7^+$ GC area with $Thy1.2^+$ staining. Counterstained with B220 to identify GC within the B cell follicle. (*A* and *B*) One experiment of three to five independent experiments, three to four mice per group/experiment. (*D* and *E*) Two independent experiments, three to four mice per group/experiment. (*F*) Acute cilengitide treatment scheme for WT mice immunized with OVA/CFA. (*G*) Representative IHC day 21 postimmunization: GL7 (red), CD35 (blue), and CD3 (green). Dotted lines, approximate GC area. (*H*) $CD3^+$ objects within the $GL7^+$ GC, number per 5,000 μm^2. Three independent experiments, four to five mice per group/experiment. Statistics by Mann–Whitney *U* test; $^*P < 0.05$, $^{**}P < 0.01$. ns, not statistically significant.

cells (ASCs) in the dLN and serum antibody levels. Early OVA-specific IgG ASCs (Fig. 6*D*) and serum IgM (Fig. 6*E*) responses were intact in the absence of T cell α_V integrin. However, over time the number of dLN OVA-IgG ASCs declined (days 21–28) (Fig. 6*D*) in immunized α_V-CD4 cKO mice and was accompanied by significant reductions in OVA-specific serum IgG concentrations (Fig. 6*F*) and a decrease in IgG affinity (Fig. 6*G*) (52). Thus, the premature decline in the GC response of α_V-deficient Tfh cells correlates with a late reduction in GC B cells and less effective selection of high-affinity GC B cells.

T Cell Integrin α_V Is Essential for LLPCs but Not Bmem Cells. An effective GC response results in the generation of LLPCs and Bmem cells (53) and has been suggested to be temporally regulated with early production of Bmem cells that transitions into a late generation of LLPCs (54). Given the attenuated kinetics of the GC response in α_V-CD4 cKO mice we postulated that the maintenance of Tfh GC location may regulate these temporally controlled events. To correlate Tfh GC accumulation with GC output of lasting memory and plasma cells in α_V-CD4 cKO mice we assessed OVA-specific B cell responses at late time points following immunization, well past the contraction of the GC reaction itself (day 64). As a measure of LLPCs we analyzed ex vivo OVA-specific ASCs in the BM (Fig. 7 *A* and *B*), and for Bmem cells splenocytes were restimulated in vitro before an OVA-specific IgG enzyme-linked immunospot (ELISPOT) assay (Fig. 7*C*). Kinetic analysis of the BM revealed a striking decrease in LLPCs when T cell support of the GC is α_V integrin-deficient (Fig. 7 *A* and *B*). In stark contrast, Bmem responses in α_V-CD4 cKO mice remained intact (Fig. 7*C*).

To extend our analysis of GC output in response to infection, we infected mice with X31 Influenza A virus and looked at LLPCs and Bmem cells on days 72–75 postinfection. There was a robust loss of HA-specific LLPCs in flu-infected α_V-CD4 cKO mice (Fig. 7*D*) similar in magnitude to that observed following OVA immunization. Moreover, the defects in LLPCs correlated with a functionally significant decrease in the ability of serum Abs to neutralize viral infectivity (*SI Appendix*, Fig. S9). Despite the dramatic defect in LLPCs in the absence of T cell α_V integrins, the generation of flu-specific Bmem cells remained intact, phenotypically (day 40) (Fig. 7*E*) (see gating strategies in *SI Appendix*, Fig. S3) and functionally (days 72–75) (Fig. 7*F*). Our results of a differential dependency for Tfh integrin α_V on Bmem versus LLPC output is consistent with a critical, and highly specific, role for integrin α_V in maintaining long-term GC positioning of Tfh in support of the mature GC reaction.

Our results support a role for the recognition of FDC-displayed ECM components in the continued maintenance of Tfh in the GC (*SI Appendix*, Fig. S10). The changes in Tfh availability in the GC in the absence of α_V integrin and concomitant loss of LLPCs are consistent with the temporal model of GC output put forth for B cells (54), suggesting sustained α_V integrin-dependent Tfh positioning in the GC is required for the late emergence of LLPCs.

Discussion

The regulation of Tfh dwell time in the GC for selection of high-affinity B cells is pivotal for robust protective immunity. We reveal a role for the matrix-binding integrin α_V in Tfh GC positioning and have connected that to the long-term support of the GC reaction. Our studies were prompted by the restricted GC expression of a number of RGD-containing ligands for integrin α_V, raising

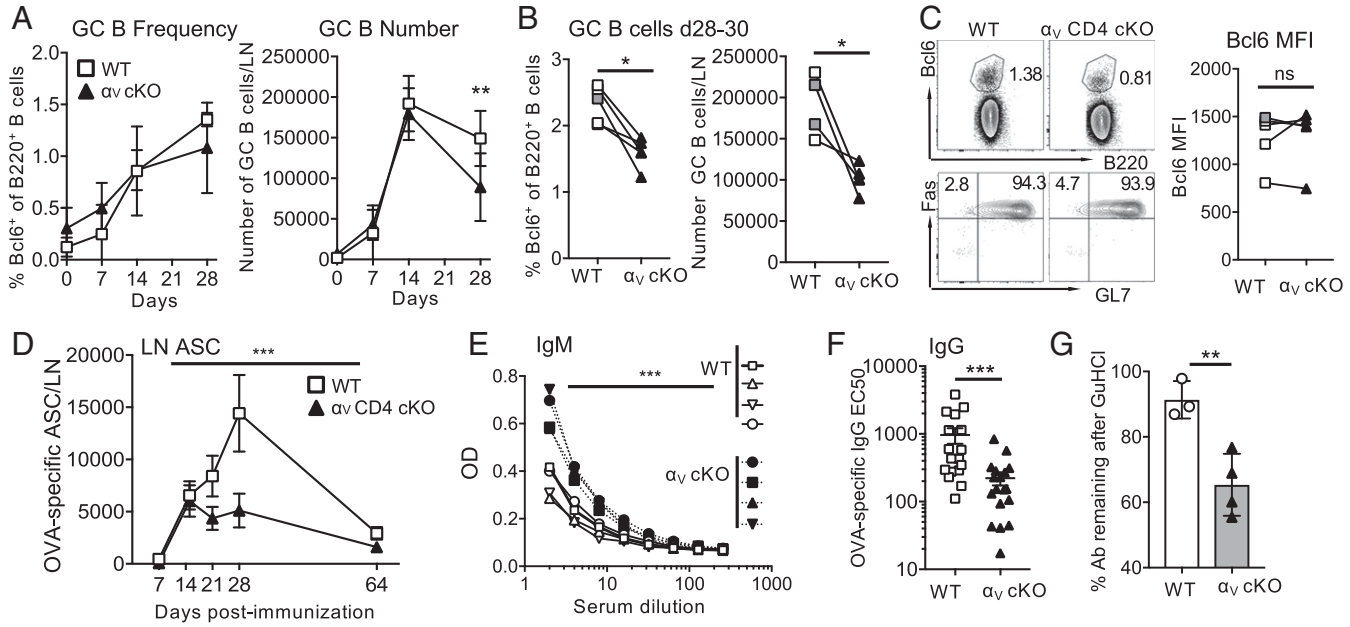

Fig. 6. Defect in GC B cell responses. (*A*) Kinetic analysis of Bcl6$^+$ GC B cell frequency and number in WT (C57BL/6) and α_V-CD4 cKO in dLN after OVA/CFA immunization. Statistics by two-tailed unpaired *t* test; $^{**}P < 0.01$. (*B*) Frequency and number of Bcl6$^+$ GC B cells on days 28–30 from five independent experiments; symbols represent the mean value from groups of four to five mice with WT and α_V-CD4 cKO groups from individual experiments paired. WT: white squares $\alpha_V^{+/+}$ CD4-Cre$^+$ littermates, gray squares C57BL/6. Statistics by paired *t* test; $^{*}P < 0.05$. (*C*) Representative plots showing Bcl6 expression on B220$^+$ B cells (*Top*) and expression of Fas and GL7 (*Bottom*), day 28. (*Right*) Bcl6 MFI d28-d30. Symbols represent the mean value from groups of four to five mice, with WT and α_V-CD4 cKO groups from individual experiments paired. WT: white squares $\alpha_V^{+/+}$ CD4-Cre$^+$ littermates, gray squares C57BL/6. Statistics by paired *t* test. (*D*) Kinetic analysis of OVA-specific IgG ASCs in dLN postimmunization/infection, WT (C57BL/6) and α_V-CD4 cKO, combined data from three independent experiments four mice per group. Statistics by two-way ANOVA; $^{***}P < 0.001$. (*E*) OVA-specific IgM in serum, day 10; symbols represent individual mice. Statistics by two-way ANOVA; $^{***}P < 0.001$. (*F*) EC_{50} of OVA-specific IgG from sera day 30 post-immunization. three independent experiments, four to five mice per group/experiment. Each symbol an individual mouse. (*G*) Loss of OVA-specific IgG binding after treatment with 1 M GuHCl. Percent OD signal remaining after treatment with GuHCl. Representative experiment of three independent experiments. (*E–G*) WT, $\alpha_V^{+/+}$ CD4-Cre$^+$ littermates. All statistics by Mann–Whitney *U* test (unless otherwise stated); $^{**}P < 0.01$, $^{***}P < 0.001$. ns, not statistically significant.

the possibility that these ligands provided spatial positioning or retention cues for effector cells in the GC. T cell integrin α_V deficiency led to failure to sustain GC size and numbers. Loss of integrin α_V did not impede Tfh generation or initial GC development but did impair Tfh GC accumulation and sustained GC reactions. Deficient Tfh GC accumulation led to a marked defect in high-affinity antibodies and in LLPCs. Conversely, the generation of Bmem cells was not dependent on Tfh α_V integrins and may instead reflect GC-independent help for Bmem development (55) or reflect a dependency for Tfh help only in the early GC response (54) when α_V-deficient Tfh are present in the GC. Thus, our results highlight a critical ECM:α_V integrin axis specifically regulating prolonged Tfh positioning within the GC and support of GC maturation for LLPC generation.

The GC is a highly dynamic structure with T and B cell movement within and between GCs. While Tfh can leave one GC and enter another (56), most Tfh remain in a single GC for days. The signals that control Tfh GC residency remain incompletely understood. Initial Tfh GC positioning requires SAP-dependent stable T:B cell contacts (16, 17) and responsiveness to LZ-produced CXCL13 (14, 15). Expression of plexin B2 by GC B cells appears to facilitate semaphorin 4C-expressing Tfh adhesion to further promote Tfh migration toward the GC center (24). In addition, restricting responsiveness to T cell zone signals CCL21 and S1P provides further control of Tfh spatial restriction to the GC (22). However, the impact of these Tfh positioning cues often has surprisingly modest effects on GC output: GC B cell responses were not reduced by S1PR2 deficiency despite a 50% reduction in Tfh GC positioning. Indeed, whether sustained recruitment or retention of Tfh is required weeks into the GC reaction is unclear. The near absence of LLPCs when T cell α_V integrins are deleted is therefore a finding that appears to suggest that sustained Tfh presence in the GC is critical for LLPC generation. Alpha V integrins play roles in cell signaling for survival and activation, adhesion, and interstitial migration and a number of these functions may be at play in regulating α_V integrin-dependent Tfh accumulation in the GC. For B cells, enriched expression of laminin α5 in the marginal zone of the spleen appears to be critical for marginal zone B cell development and/or survival (57). Whether ECM–α_V integrin interactions also provide signals for Tfh functional maturation or survival within the GC will be critical to assess in future studies. We favor a model where FDC presentation of α_V integrin ligands provides a physical adhesion-based retention cue for Tfh in the LZ, lengthening GC dwell time (*SI Appendix*, Fig. S10). Interestingly, while α_V integrin-dependent GC positioning appears to be T cell-intrinsic, based on the GC mislocation of transferred α_V-deficient OT-II T cells on day 10, the iterative defects in GC accumulation in a polyclonal response appear to be spatially and functionally compounded with time, evident late (but not early) in the GC response. This could mean that temporal changes in the number of Tfh cells in the GC may differentially impact GC output or that there is a temporally regulated Tfh functional switch that is required to support the late GC generation of LLPCs.

The FDCs in the GC are part of the stromal network in the LN and are closely related to the FRC network in the T cell zone (58). GC B cells move along antigen-loaded FDC processes (5, 59, 60) and α_V integrin-mediated adhesion/migration of Tfh to the same FDC network may optimize GC T:B cell encounter,

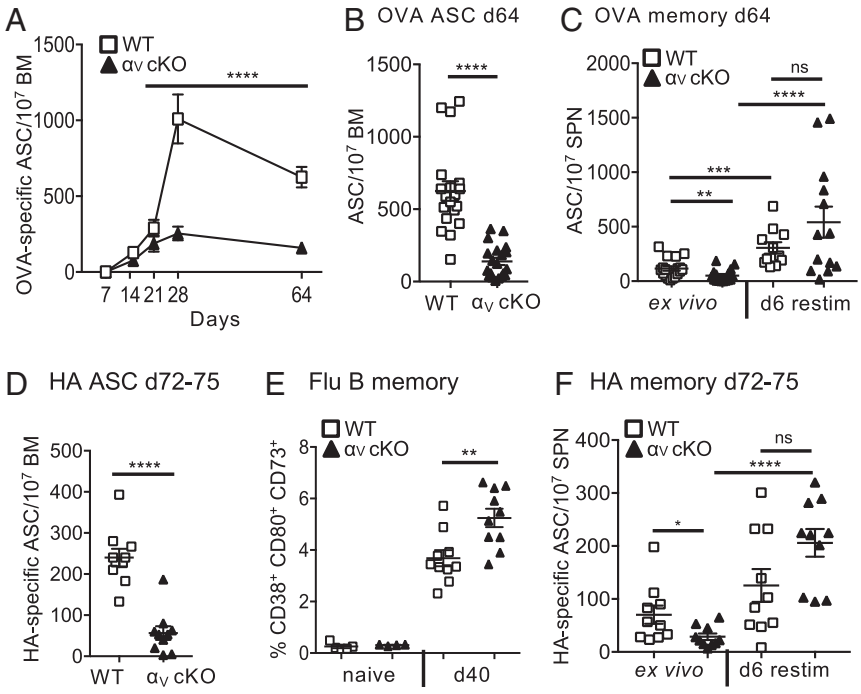

Fig. 7. Specific defect in LLPCs in the absence of Tfh integrin α_V. (*A*) Kinetic analysis of OVA-specific IgG ASCs in BM postimmunization. WT (C57BL/6) and α_V-CD4 cKO, combined data from three independent experiments four mice per group. Statistics by two-way ANOVA; ****$P < 0.0001$. (*B*) OVA IgG ASCs in BM day 64, individual mice from *A*. (*C*) OVA-specific IgG ELISPOTS from Bmem cells in spleen (SPN) day 65 postimmunization: ex vivo and following 6-d restimulation with LPS. (*D*) HA-specific IgG ASCs in BM days 72–75 after X31 influenza infection. (*E*) Frequency of Bmem cells ($CD19^+CD4^-CD38^+CD80^+CD73^+$) in dLN by flow cytometry in naïve and flu-infected mice, day 40 (WT, $\alpha_V^{+/+}$ CD4-Cre$^+$ littermates). (*F*) HA-specific IgG ELISPOTS from Bmem cells in spleen (SPN) days 72–75 postinfection: ex vivo and following 6-d restimulation. Two to three independent experiments, five mice per group/experiment. All statistics by Mann–Whitney *U* test (unless otherwise stated); *$P < 0.05$, **$P < 0.01$, ***$P < 0.001$, ****$P < 0.0001$. Each symbol represents an individual mouse. ns, not statistically significant.

akin to promotion of T:DC contacts along the FRC (61–63). Indeed, physical Tfh:FDC interactions have been evoked to explain the proposed "hand-off" of HIV from FDC to Tfh (58, 64). ECM–α_V integrin interactions between Tfh and FDC may also facilitate the active motility seen in the GC LZ (46, 65), similar to the α_V-dependent contact guidance of T cells along matrix fibers in the inflamed skin (40).

The disconnect between Bmem and LLPC production that we observe with α_V integrin deficiency in T cells raises interesting questions of temporal requirements for Tfh help. Bmem cells appear to arise early in the GC response and can also develop in a T-dependent manner that is independent of the GC (54, 55). The presence of Bmem and the specific absence of LLPC that is associated with Tfh α_V deficiency points to a niche-specific role for α_V integrins in the GC itself, rather than a defect in the ability to provide B cell help per se. These studies also raise fundamental questions surrounding the temporal requirements for Tfh over the many weeks that constitute a GC reaction. This α_V:ECM Tfh checkpoint could have broad therapeutic application for enhancing or diminishing plasma cell responses and Tfh-related pathologies.

Materials and Methods

Mice and Immunizations. All mice were bred and maintained in the pathogen-free animal facility at the University of Rochester. *itgav*$^{fl/fl}$ mice were generated in a 129/Ola background and back-crossed 10 generations to C57BL/6J (66). C57BL/6J *itgav*$^{fl/fl}$ mice were crossed to C57BL/6J CD4-Cre mice (JAX) (34) and *itgav*$^{wt/wt}$ CD4-Cre$^+$ littermates used as WT controls, unless otherwise specified. All animal procedures were approved by the Institutional Animal Care and Use Committee of the University of Rochester. Mice were immunized i.d. in the ear with 1 μg OVA protein in CFA.

IHC. Eight-micrometer frozen sections were stained for the indicated markers (*SI Appendix*) and images processed in ImageJ. Three to four sections across the center of each LN were collected and analyzed. Confocal images were acquired using a FluoView FV1000 Laser Scanning Confocal Microscope (Olympus). Fifteen-micrometer z-stacks with 1.64-μm spacing between slices were taken with a 20× oil immersion objective lens. Confocal image analysis was done using Imaris (Bitplane). Three-dimensional surfaces were generated from individual channels in the Imaris surface tool (1.25-μm smoothing tool and a minimum cutoff of 10 voxels). Overlap was determined by masking corresponding channels and removing non-overlapping voxels. Remaining overlapping voxels are displayed as an independent surface (white).

Antibodies and Flow Cytometry. All Abs were from BD, Biolegend, or eBioscience: Live/Dead (Invitrogen), CD16/CD32 antibody (2.4G2), CD4 (RM4-5), CD44 (IM7), CXCR5 (2G8), PD1 (J43), ICOS (C398.4A), Bcl6 (K112-91), CD138 (281-2), CD19 (1D3), B220 (RA3 6B2), GL7 (GL7), CD95 (Jo2), Thy1.2 (30-H12), alpha V (Hma5-1), CD73 (TY/11.8), CD80 (16-10A1), CD38 (90/CD38), CD90.2 (53-2.1), CD90.1(OX-7), IgMα(DS-1), and IgD(11-26c.2a). All flow cytometric analysis was performed on BD LSR-II or BD LSR-Fortessa machines.

CD4+ T Cell Transfer. Purified naïve OT-II T cells (5×10^5) were transferred i.v. to Thy1.1$^+$ C57BL/6 recipients and recipient mice immunized with OVA/CFA 12 h after cell transfer. For LN homing studies in nonimmunized mice, 1×10^6 naïve OT-II T cells were transferred.

In Vivo-Generated Tfh. LN cells were FACS-sorted for Tfh ($CD19^-CD4^+$ $CD44^{high}$ $CXCR5^+$ PD-1$^+$) and non-Tfh ($CD19^-$ $CD4^+$ $CD44^{high}$ $CXCR5^-$ PD-1$^-$).

Serum Antibody ELISA. ELISA plates were coated with OVA protein and incubated overnight with serum samples. Antibody affinity was measured using a published technique (52).

T:B Cell Adhesion. LPS-stimulated B cells were loaded with OVA peptide (323–339) (0.2 to 20 μM); 500,000 B cells and 165,000 T cells were pelleted and incubated at 37 °C for 30 min before fixation. Frequency of T cells in conjugates represents fraction of CD4+CD19+ events of the total CD4s by FACS.

B Cell Maturation and IgG Production. Thirty thousand ex vivo Tfh were cocultured with 50,000 resting B cells ±2 μg/mL anti-CD3 (2C11) and anti-mouse-IgM. On day 6, cells were stained for GL7 for flow cytometry. Tfh were cultured at a 1:1 ratio with resting B cells. On day 11 supernatants were assayed for IgG by ELISA.

In Vivo B Cell Help. Resting MD4 B cells (1×10^5) were adoptively transferred with/without 1×10^5 naïve OT-II $CD4^+$ T cells to MOG-specific 2D2 TCR Tg+ mice (JAX). Mice were immunized with 3.3 μg HEL-OVA in CFA and dLN harvested for flow cytometric analysis on day 5 postimmunization.

Acute $\alpha_V\beta_3$ Blockade. WT C57BL/6 mice were immunized with OVA/CFA and given 100 μg cilengitide trifluoroacetate (Sigma Life Science) i.p. daily on days 17–20 and mice were killed on day 21 for IHC of dLN. The vehicle was 1% DMSO.

Influenza A Infection. H3N2 A/Hong Kong/X31 (X31) influenza virus was grown and titered in embryonated chicken eggs. Allantoic fluid was diluted in PBS and used to infect mice intranasally (10^5 50% egg infective dose in 30 μL).

B Cell ELISPOT. BM, SPN, or dLN cells, directly ex vivo, were incubated for 3 to 4 h on OVA protein-, X-31 HA-, or BSA-coated plates. ASC spots were detected with anti-IgG biotin. For Bmem, SPN cells were stimulated with 5 μg/mL LPS and 10 U/mL rhIL-2 for 6 d before the OVA- or HA-specific ELISPOT.

ACKNOWLEDGMENTS. We thank members of the D.J.F. laboratory for helpful discussions and the Topham laboratory (University of Rochester) for providing X31 influenza virus. This work was supported by National Institutes of Health/National Institute of Allergy and Infectious Diseases Grants P01 AI02851 (to D.J.F.), T32 AI007285-28 (to D.C.S.), and T90 DE021985 (to S.A.L.).

1. Crotty S, Ahmed R (2004) Immunological memory in humans. *Semin Immunol* 16: 197–203.
2. De Silva NS, Klein U (2015) Dynamics of B cells in germinal centres. *Nat Rev Immunol* 15:137–148.
3. Victora GD, Nussenzweig MC (2012) Germinal centers. *Annu Rev Immunol* 30: 429–457.
4. Bannard O, Cyster JG (2017) Germinal centers: Programmed for affinity maturation and antibody diversification. *Curr Opin Immunol* 45:21–30.
5. Allen CD, Okada T, Tang HL, Cyster JG (2007) Imaging of germinal center selection events during affinity maturation. *Science* 315:528–531.
6. Victora GD, et al. (2010) Germinal center dynamics revealed by multiphoton microscopy with a photoactivatable fluorescent reporter. *Cell* 143:592–605.
7. Mesin L, Ersching J, Victora GD (2016) Germinal center B cell dynamics. *Immunity* 45: 471–482.
8. Batista FD, Neuberger MS (2000) B cells extract and present immobilized antigen: Implications for affinity discrimination. *EMBO J* 19:513–520.
9. Gitlin AD, et al. (2015) HUMORAL IMMUNITY. T cell help controls the speed of the cell cycle in germinal center B cells. *Science* 349:643–646.
10. Gitlin AD, Shulman Z, Nussenzweig MC (2014) Clonal selection in the germinal centre by regulated proliferation and hypermutation. *Nature* 509:637–640.
11. Dufaud CR, McHeyzer-Williams LJ, McHeyzer-Williams MG (2017) Deconstructing the germinal center, one cell at a time. *Curr Opin Immunol* 45:112–118.
12. Qi H (2016) T follicular helper cells in space-time. *Nat Rev Immunol* 16:612–625.
13. Vinuesa CG, Linterman MA, Yu D, MacLennan IC (2016) Follicular helper T cells. *Annu Rev Immunol* 34:335–368.
14. Haynes NM, et al. (2007) Role of CXCR5 and CCR7 in follicular Th cell positioning and appearance of a programmed cell death gene-1high germinal center-associated subpopulation. *J Immunol* 179:5099–5108.
15. Hardtke S, Ohl L, Förster R (2005) Balanced expression of CXCR5 and CCR7 on follicular T helper cells determines their transient positioning to lymph node follicles and is essential for efficient B-cell help. *Blood* 106:1924–1931.
16. Qi H, Cannons JL, Klauschen F, Schwartzberg PL, Germain RN (2008) SAP-controlled T-B cell interactions underlie germinal centre formation. *Nature* 455:764–769.
17. Cannons JL, et al. (2010) Optimal germinal center responses require a multistage T cell:B cell adhesion process involving integrins, SLAM-associated protein, and CD84. *Immunity* 32:253–265.
18. Takahashi Y, Dutta PR, Cerasoli DM, Kelsoe G (1998) In situ studies of the primary immune response to (4-hydroxy-3-nitrophenyl)acetyl. V. Affinity maturation develops in two stages of clonal selection. *J Exp Med* 187:885–895.
19. Grammer AC, et al. (2003) Abnormal germinal center reactions in systemic lupus erythematosus demonstrated by blockade of CD154-CD40 interactions. *J Clin Invest* 112: 1506–1520.
20. Chen J, et al. (2013) Reversing endogenous alloreactive B cell GC responses with anti-CD154 or CTLA-4Ig. *Am J Transplant* 13:2280–2292.
21. Green JA, et al. (2011) The sphingosine 1-phosphate receptor $S1P_2$ maintains the homeostasis of germinal center B cells and promotes niche confinement. *Nat Immunol* 12:672–680.
22. Moriyama S, et al. (2014) Sphingosine-1-phosphate receptor 2 is critical for follicular helper T cell retention in germinal centers. *J Exp Med* 211:1297–1305.
23. Lu P, Shih C, Qi H (2017) Ephrin B1-mediated repulsion and signaling control germinal center T cell territoriality and function. *Science* 356:eaai9264.
24. Yan H, et al. (2017) Plexin B2 and semaphorin 4C guide T cell recruitment and function in the germinal center. *Cell Rep* 19:995–1007.
25. Sorokin L (2010) The impact of the extracellular matrix on inflammation. *Nat Rev Immunol* 10:712–723.
26. Chang JE, Turley SJ (2015) Stromal infrastructure of the lymph node and coordination of immunity. *Trends Immunol* 36:30–39.
27. Sobocinski GP, et al. (2010) Ultrastructural localization of extracellular matrix proteins of the lymph node cortex: Evidence supporting the reticular network as a pathway for lymphocyte migration. *BMC Immunol* 11:42.
28. Halstensen TS, Mollnes TE, Brandtzaeg P (1988) Terminal complement complex (TCC) and S-protein (vitronectin) on follicular dendritic cells in human lymphoid tissues. *Immunology* 65:193–197.
29. Wang X, Rodda LB, Bannard O, Cyster JG (2014) Integrin-mediated interactions between B cells and follicular dendritic cells influence germinal center B cell fitness. *J Immunol* 192:4601–4609.
30. Krautler NJ, et al. (2012) Follicular dendritic cells emerge from ubiquitous perivascular precursors. *Cell* 150:194–206.
31. Li Q, et al. (2005) Potential roles of follicular dendritic cell-associated osteopontin in lymphoid follicle pathology and repair and in B cell regulation in HIV-1 and SIV infection. *J Infect Dis* 192:1269–1276.
32. Savill J, Dransfield I, Hogg N, Haslett C (1990) Vitronectin receptor-mediated phagocytosis of cells undergoing apoptosis. *Nature* 343:170–173.
33. Albert ML, et al. (1998) Immature dendritic cells phagocytose apoptotic cells via alphavbeta5 and CD36, and cross-present antigens to cytotoxic T lymphocytes. *J Exp Med* 188:1359–1368.
34. Acharya M, et al. (2010) αv integrin expression by DCs is required for Th17 cell differentiation and development of experimental autoimmune encephalomyelitis in mice. *J Clin Invest* 120:4445–4452.
35. Travis MA, et al. (2007) Loss of integrin alpha(v)beta8 on dendritic cells causes autoimmunity and colitis in mice. *Nature* 449:361–365.
36. Melton AC, et al. (2010) Expression of αvβ8 integrin on dendritic cells regulates Th17 cell development and experimental autoimmune encephalomyelitis in mice. *J Clin Invest* 120:4436–4444.
37. Gerold G, et al. (2008) A toll-like receptor 2-integrin beta3 complex senses bacterial lipopeptides via vitronectin. *Nat Immunol* 9:761–768.
38. Gianni T, Leoni V, Chesnokova LS, Hutt-Fletcher LM, Campadelli-Fiume G (2012) αvβ3-integrin is a major sensor and activator of innate immunity to herpes simplex virus-1. *Proc Natl Acad Sci USA* 109:19792–19797.
39. Acharya M, et al. (2016) αv integrins combine with LC3 and atg5 to regulate toll-like receptor signalling in B cells. *Nat Commun* 7:10917.
40. Overstreet MG, et al. (2013) Inflammation-induced interstitial migration of effector $CD4^+$ T cells is dependent on integrin αV. *Nat Immunol* 14:949–958.
41. Du F, et al. (2016) Inflammatory Th17 cells express integrin αvβ3 for pathogenic function. *Cell Rep* 16:1339–1351.
42. Castaños-Velez E, Biberfeld P, Patarroyo M (1995) Extracellular matrix proteins and integrin receptors in reactive and non-reactive lymph nodes. *Immunology* 86: 270–278.
43. Acton SE, et al. (2012) Podoplanin-rich stromal networks induce dendritic cell motility via activation of the C-type lectin receptor CLEC-2. *Immunity* 37:276–289.
44. Meli AP, et al. (2016) The integrin LFA-1 controls T follicular helper cell generation and maintenance. *Immunity* 45:831–846.
45. Choi YS, et al. (2011) ICOS receptor instructs T follicular helper cell versus effector cell differentiation via induction of the transcriptional repressor Bcl6. *Immunity* 34:932–946.
46. Liu D, et al. (2015) T-B-cell entanglement and ICOSL-driven feed-forward regulation of germinal centre reaction. *Nature* 517:214–218.
47. Ramiscal RR, Vinuesa CG (2013) T-cell subsets in the germinal center. *Immunol Rev* 252:146–155.
48. Sage PT, Sharpe AH (2016) T follicular regulatory cells. *Immunol Rev* 271:246–259.
49. Chu C, et al. (2014) SAP-regulated T cell-APC adhesion and ligation-dependent and -independent Ly108-CD3ζ interactions. *J Immunol* 193:3860–3871.
50. Mas-Moruno C, Rechenmacher F, Kessler H (2010) Cilengitide: The first anti-angiogenic small molecule drug candidate design, synthesis and clinical evaluation. *Anticancer Agents Med Chem* 10:753–768.
51. Wong PP, et al. (2015) Dual-action combination therapy enhances angiogenesis while reducing tumor growth and spread. *Cancer Cell* 27:123–137.
52. Dauner JG, et al. (2012) Development and application of a GuHCl-modified ELISA to measure the avidity of anti-HPV L1 VLP antibodies in vaccinated individuals. *Mol Cell Probes* 26:73–80.
53. Nutt SL, Hodgkin PD, Tarlinton DM, Corcoran LM (2015) The generation of antibody-secreting plasma cells. *Nat Rev Immunol* 15:160–171.
54. Weisel FJ, Zuccarino-Catania GV, Chikina M, Shlomchik MJ (2016) A temporal switch in the germinal center determines differential output of memory B and plasma cells. *Immunity* 44:116–130.
55. Weisel F, Shlomchik M (2017) Memory B cells of mice and humans. *Annu Rev Immunol* 35:255–284.
56. Shulman Z, et al. (2013) T follicular helper cell dynamics in germinal centers. *Science* 341:673–677.
57. Song J, et al. (2013) Extracellular matrix of secondary lymphoid organs impacts on B-cell fate and survival. *Proc Natl Acad Sci USA* 110:E2915–E2924.
58. Heesters BA, Myers RC, Carroll MC (2014) Follicular dendritic cells: Dynamic antigen libraries. *Nat Rev Immunol* 14:495–504.

59. Schwickert TA, et al. (2007) In vivo imaging of germinal centres reveals a dynamic open structure. *Nature* 446:83–87.
60. Hauser AE, et al. (2007) Definition of germinal-center B cell migration in vivo reveals predominant intrazonal circulation patterns. *Immunity* 26:655–667.
61. Bajénoff M, et al. (2007) Highways, byways and breadcrumbs: Directing lymphocyte traffic in the lymph node. *Trends Immunol* 28:346–352.
62. Brown FD, Turley SJ (2015) Fibroblastic reticular cells: Organization and regulation of the T lymphocyte life cycle. *J Immunol* 194:1389–1394.
63. Denton AE, Linterman MA (2017) Stromal networking: Cellular connections in the germinal centre. *Curr Opin Immunol* 45:103–111.
64. Perreau M, et al. (2013) Follicular helper T cells serve as the major CD4 T cell compartment for HIV-1 infection, replication, and production. *J Exp Med* 210:143–156.
65. Shulman Z, et al. (2014) Dynamic signaling by T follicular helper cells during germinal center B cell selection. *Science* 345:1058–1062.
66. Lacy-Hulbert A, et al. (2007) Ulcerative colitis and autoimmunity induced by loss of myeloid alphav integrins. *Proc Natl Acad Sci USA* 104:15823–15828.